Energy Management Strategy for Grid-tied Microgrids considering the Energy Storage Efficiency

Wu, Ji; Xing, Xiaowen; Liu, Xingtao; Guerrero, Josep M.; Chen, Zonghai

Published in:
IEEE Transactions on Industrial Electronics

DOI (link to publication from Publisher):
10.1109/TIE.2018.2818660

Publication date:
2018

Document Version
Accepted author manuscript, peer reviewed version

Energy Management Strategy for Grid-tied Microgrids considering the Energy Storage Efficiency

Ji Wu, *Student Member*, *IEEE*, Xiaowen Xing, Xingtao Liu, Josep M. Guerrero, *Fellow*, *IEEE*, and Zonghai Chen, *Member*, *IEEE*

***Abstract*—A grid-tied micro-grid (MG) with the battery energy storage system (BESS) is studied in this paper. The energy storage efficiencies of the BESS are considered to optimize the operational cost of the MG. Two quadratic functions are verified and utilized to formulate the efficiencies of BESS in both charge and discharge process. Afterwards, constraints of MG power scheme are investigated based on aforementioned equations. Furthermore, the 24-hour ahead forecasting data of photovoltaic (PV) generation and loads demand are also utilized during MG modeling. To minimize the operational electricity cost of the MG in the next 24 hours, a nonlinear programming with discontinuous derivatives (DNLP) solver is applied based on the proposed constraints. Additionally, to balance the power flow of MG and reduce the effects of the forecasting error of PV generation, a two steps MG management strategy is therefore developed based on the scheduled power. Experiments are conducted to verify the relationship between battery energy storage efficiency and charging/discharging current of the lithium-ion battery. Moreover, the proposed energy management strategy is validated by the hardware-in-the-loop (HIL) experiments for real-time MG operation.**

***Index Terms*—Microgrids, lithium-ion battery, energy storage efficiency, energy management, nonlinear programming.**

I. Introduction

THE last decade has witnessed a considerable improvement in the research and application of the MGs [1], [2]. Different types of renewable energy sources (RESs), such as PV, wind and geothermal, have been developed and applied in the MGs to reduce electricity cost and environmental pollution. In the meanwhile, due to the uncertainty of these RES, energy storage systems (ESSs) including: batteries, flywheels and so on, have been widely used in the MGs. Hence, the power quality and system stability can be guaranteed. Furthermore, to control the RESs and ESSs, schedule the power flow of the MG and optimize the energy cost, droop control based hierarchical control has been therefore proposed [3]-[5]. In the first level (primary control) and second level (secondary control) of the MG, the voltage and frequency of the system are ensured through the control of power electronics devices. Moreover, the optimal energy management strategy is usually developed in the third level (tertiary control) to reduce cost and increase reliability.

ESS is playing a particularly important role in the MGs nowadays. The redundant energy of the RESs may be stored in the ESS in order to restrain the power fluctuation and save electricity cost. As an environmentally friendly energy storage device with high energy density and long-serving lifetime, lithium-ion battery has gained significant attention in recent years [6]-[8]. State of the battery would directly impact the operation and management of the MGs. In order to monitor battery's real-time status and protect it from hazardous operations, battery management system (BMS) is therefore proposed. To depict the remaining capacity of the battery, state of charge (SoC) is presented [9]. Furthermore, other states like residual energy, peak power capability, and remaining time to discharge of the battery can also be estimated based on SoC by the BMS [10]-[13]. Additionally, since the charging and discharging processes of a battery are the conversions between electric energy and chemical energy, energy conversion efficiency of the battery is particularly important in real applications. In [14] and [15], the efficiency of the battery is set to a constant value for both charging and discharging. Efficiencies of charge and discharge are assumed to be different in [16] and [17] which may be more reasonable. More scientifically, Lee [18] employed a discharging current considered equation to compute the efficiency of the battery energy storage system (BESS). However, battery energy storage efficiency during the charging process has not been fully discussed.

After analyzing the properties of the RESs and ESSs, power flow optimization strategy for the MGs may be developed by

This work was supported in part by the National Natural Science Fund of China under Grant 61375079 and in part by the China Scholarship Council under No. 201606340099. (corresponding author: Zonghai Chen).

Ji Wu and Zonghai Chen are with Department of Automation, University of Science and Technology of China, 230027 Hefei, PR China (e-mail: chnwuji@mail.ustc.edu.cn, chenzh@ustc.edu.cn)

Xiaowen Xing is with Department of Automation, Northwestern Polytechnical University, 710065 Xi'an, PR China (e-mail: xingxiaowen136@126.com).

Xingtao Liu is with School of Automotive and Traffic Engineering, Hefei University of Technology, 230000 Hefei, PR China (e-mail: xingtao.liu@hfut.edu.cn).

Josep M. Guerrero is with Department of Energy Technology, Aalborg University, 9220 Aalborg, Denmark (e-mail: joz@et.aau.dk).

This article has been accepted for publication in a future issue of this journal, but has not been fully edited. Content may change prior to final publication. Citation information: DOI 10.1109/TIE.2018.2818660, IEEE Transactions on Industrial Electronics

the energy management system (EMS). Mathematical models of the generators and storage systems, e.g., voltage source converter, PV, battery, fuel cell, were proposed for the optimal operation of an isolated MG in [19]. In [20], the range of battery charge/discharge SoC and the boundaries of input/output power were listed as constraints during the modeling of MG. Afterwards, operation cost minimization of the MG was figured out by a mixed integer linear programming approach. The uncertainty of the magnitude and capacity of the MG energy output has been considered, and then solved by the chance constrained programming based frameworks in [21]. Electricity cost of a residential MG was minimized by a mixed iterative adaptive dynamic programming algorithm in [22], where the efficiencies of the BESS in MG during charging and discharging were computed according to the power output of the battery. However, forecasting error caused by the uncertainty of the RESs were not considered during the optimizing process in most of the above-mentioned researches.

Disadvantages still exist in some of the aforementioned energy management strategies. Energy storage efficiencies of the BESS during charging and discharging were not fully discussed and implemented in the model of MG. To address these issues, particular attention was paid to the relationships between battery energy storage efficiency and the input/output current. In this paper, the 1st order RC model and charge/discharge properties of the battery are firstly illustrated to qualitatively analyze of the battery efficiency. Experiments are conducted to help to analyze the magnitude of energy loss during the operation of the lithium-ion battery and build an accurate model for battery efficiency formulation. Moreover, effects of the battery efficiency on the energy management of MG and the protection of BESS are investigated through comparative experiments. Furthermore, in order to reduce the influence of RESs' forecasting errors, a two steps strategy for energy management of the MG is employed. The first step focuses on the programming of different RESs and ESSs in order to minimize the electricity cost during the operation of MG. And the second step aims to balance the power flow and reduce the impacts of the forecasting errors based on the rule summarized from the scheduled power reference.

The rest of the paper is organized as follows. Section II describes the configuration of the grid-tied AC MG in this case. Energy storage efficiency of the lithium-ion battery is discussed in Section III. Then, the bi-level energy management strategy for the grid-tied MG is introduced in Section IV. Experiments about BESS efficiency are conducted in Section V, where results of the simulation and hardware in the loop experiment are also analyzed in order to validate the proposed energy management strategy. The conclusion is given in Section VI.

II. Configuration of the Grid-tied MG

The MG in this paper is operating on a grid-tied mode based on the hierarchical control. In this mode, the power can be delivered from the utility grid to the loads or BESS through the feeder bus. Furthermore, PV and BESS are the other energy sources in this MG, while BESS can also serve as a load. As shown in Fig. 1, power electronics converters are utilized for interconnection of the utility grid, RES, BESS, and loads. Since the voltage and frequency of the AC bus can be guaranteed by the primary and secondary control of the MG [20], therefore, these issues will not be discussed in this paper. The proposed energy management strategy is applied in the tertiary control. Moreover, PV array converters are operating on the maximum power point tracking method under varying environments.

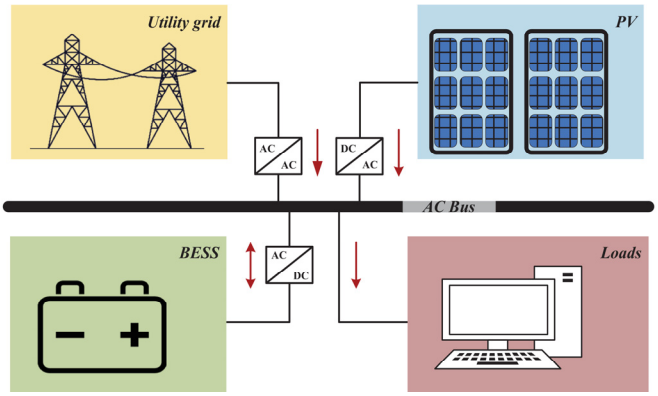

Fig. 1. A grid-tied AC MG.

TABLE I

Technical Parameters of the Lithium-ion Battery Cell

Parameter	Value
Nominal capacity [Ah]	10
Voltage range [V]	2.0 to 3.65
Maximum continuous discharging current	3 C (30 A)
Maximum continuous charging current	1 C (10 A)
Discharging temperature range [°C]	-20 to 55
Charging temperature range [°C]	0 to 45

The rated voltage and frequency of the AC bus is 220 V and 50 Hz RMS respectively. Maximum power of the PV system is about 6 kW. Lithium-ion battery cell is used in the BESS with a nominal capacity of 10 Ah, and properties of the cells are assumed to be identical. The nominal energy of the BESS is 30 kWh.

Non-dispatchable loads are applied in this MG. Hence, to minimize the electricity cost, the utilization of the renewable energy and the efficiency of the BESS should be maximized. Thus, properties of the PV system and BESS may be considered during the development and execution of the energy management strategy.

III. Characterization of the Lithium-ion Battery

Generally, BESS is composed of a few lithium-ion battery cells to supply more energy and power. Since the inconsistency of the battery cells can be reduced before battery pack assembling, hence, imbalance of the cells in the BESS will not be considered in this paper. Thus, properties of the battery cell are investigated instead of the BESS. The lithium-ion battery cell studied in this paper is manufactured by Guoxuan High-Tech Co., Ltd. in Hefei, China. In order to have a general concept of the battery cell, its performance parameters are listed in Table I.

This article has been accepted for publication in a future issue of this journal, but has not been fully edited. Content may change prior to final publication. Citation information: DOI 10.1109/TIE.2018.2818660, IEEE Transactions on Industrial Electronics

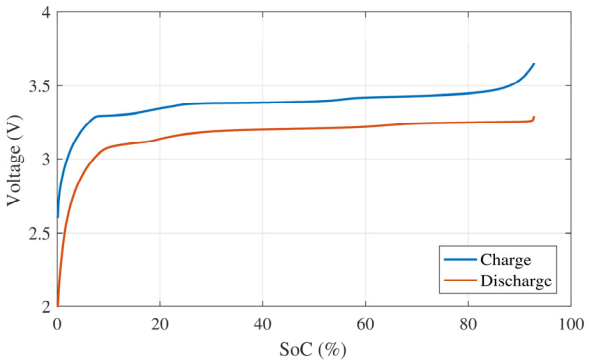

Fig. 2. Terminal voltage during charging and discharging process.

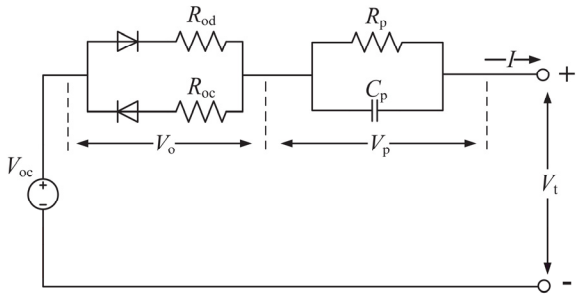

Fig. 3. Equivalent circuit model of the lithium-ion battery.

A. Terminal Voltage

The terminal voltage of the lithium-ion battery cell would be changed with the different SoC. Curves of battery terminal voltage with 0.5 C charging/discharging current are depicted in Fig. 2. It is evident that the terminal voltage during charging process is higher than the discharging process at same SoC. Moreover, for the lithium-ion used in this paper, the terminal voltage curve usually has a plateau within the SoC range of [20%, 80%]. The changing rate in this area is much smaller than the initial and terminative part of the charging/discharging process.

The 1st order resistance-capacitance (RC) model is employed to simulate the terminal voltage of the lithium-ion battery in this paper. As Fig. 3 shows, battery terminal voltage, V_t, is composed of three parts: the open circuit voltage (OCV), V_{oc}, the voltage drop caused by the Ohmic resistance, V_o, and the polarization voltage, V_p.

According to [23], the OCV can be expressed as a function of the SoC, given as follows:

$$V_{oc} = K_1 + K_2 \cdot SoC + K_3 \cdot SoC^2 + K_4 \cdot SoC^3 + K_5 / SoC + K_6 \cdot \ln(SoC) + K_7 \cdot \ln(1 - SoC) \quad (1)$$

being

$$SoC(k+1) = SoC(k) - \frac{\eta \cdot I \cdot \Delta t}{C_N}$$

where K_i (i = 1…7) are constants of the equation; $SoC(k+1)$ and $SoC(k)$ are the SoC at $(k+1)$th and kth sampling time respectively; η stands for the Columbic efficiency; Δt is the sampling interval; C_N is the nominal capacity.

The voltage drop and the polarization voltage according to Fig. 3 can be described as:

TABLE II

ENERGY OF DIFFERENT OPERATIONS

Operation	Energy (Wh)
Fully charged with constant 0.3 C	35.43
Fully discharged with constant 0.3 C	32.72
Fully discharged with constant 0.5 C	31.95

$$V_o = \begin{cases} I \cdot R_{od} & \text{when discharging} \\ I \cdot R_{oc} & \text{when charging} \end{cases} \quad (2)$$

$$\dot{V}_p = -1/C_p R_p \cdot V_p + 1/C_p \cdot I \quad (3)$$

where I is the current flowing through the battery which is assumed to be positive when discharging and negative when charging; R_{oc} and R_{od} are the Ohmic resistances used for charging and discharging processes respectively; C_p is the polarization capacitance, and R_p is the polarization resistance.

Thus, the terminal voltage of a lithium-ion battery cell can be calculated as follows:

$$V_t = V_{oc} - V_p - V_o \quad (4)$$

B. Energy Storage Efficiency

According to the aforementioned difference between battery terminal voltage values during charging and discharging at same SoC, it can be deduced that battery would input more energy than its output energy if charged capacity was equal to the discharged capacity. For instance, the energy used for battery charging from 0% SoC to 40% SoC is higher than battery output energy when SoC decrease from 40% to 0%. Therefore, energy storage loss of the lithium-ion battery is evidently existing.

As can be seen from Table II, the battery should inject about 35 Wh in order to get fully charged with a current of 0.3 C. However, with the same current value, it can output 32.72 Wh during discharging process. Furthermore, the output energy would be smaller if the discharging current increased to 0.5 C. Therefore, the energy storage efficiency of the lithium-ion battery is directly influenced by the operation status and the current value. Thus, two kinds of efficiency are defined in this paper: charging efficiency and discharging efficiency. Moreover, the definition formulas are given as follows:

$$\eta_c(I_c) = E_i / E_c(I_c) \quad (5)$$

$$\eta_d(I_d) = E_d(I_d) / E_i \quad (6)$$

where η_c and η_d are the energy storage efficiencies for charging and discharging respectively; $E_c(I_c)$ and $E_d(I_d)$ are the charged and discharged energy of the battery with current values of I_c and I_d; E_i is the stored energy inside the battery, which is also regarded as the referential energy here. In this paper, efficiencies at every SoC points are assumed to be equal.

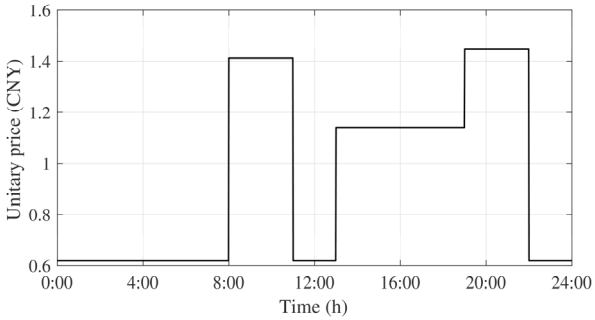

Fig. 4. Electricity price in one day.

According to the equivalent circuit model of the battery, energy losses should be a quadratic equation of the current. Thus, η_c and η_d may also have second-order relations with the current flowing through the battery. Experiments are conducted in Section V to verify the relation formulas and identify their parameters.

IV. Proposed Energy Management Strategy

In order to minimize the electricity costs of the MG, an energy management strategy is developed based on the analysis of RES, ESS, and loads.

A. Objective Function

As a grid-tied MG, the main objective of the EMS is to reduce the operational electricity cost. Since the costs of planning, installation, and maintenance, e.g., the expenditures for purchasing PV panels, battery system, and converters, are sunk costs, they could not be changed by the proposed energy management strategy which is developed for optimizing the operational cost of the MG. Thus these costs will not be considered in this paper. Due to several unfathomed technical problems, e.g. power quality degradation, injecting power generation from the MG to the utility grid is not allowed in this paper. Thus, the objective function can be expressed as follows:

$$J_c = \sum_{t=1}^{\mathrm{T}} E_g(t) \cdot f_p(t) \tag{7}$$

being

$$E_g(t) = P_g(t) \cdot \Delta t$$

where J_c is the total cost during the period T, which is equal to 24 hours here; E_g is the injected energy from the utility grid at tth optimizing time; f_p represents the unitary cost of the electricity, and it is a time-of-use (TOU) rate plan for industrial users as shown in Fig. 4; P_g is the output power of the grid; Δt is the unitary optimizing time, which is set to 15 min. in this paper.

As shown in Fig. 4, the TOU tariff means that electricity costs different price at different periods of the day. Therefore, in order to minimize the electricity cost in one typical day, electricity trades to the grid should be reduced during the peak periods, which are [8:00, 11:00] and [19:00, 22:00].

B. Constraints

In order to obtain an optimal result for MG operation, (7) is minimized according to several constraints, such as energy balance, BESS output power bound, BESS internal energy balance, etc.

Firstly, the demand of the consumers in the MG should be satisfied by the energy sources all the optimizing period. Moreover, efficiencies of the DC and AC converters are assumed to be constant. Hence, the expression can be written as follows:

$$E_g(t) \cdot \eta_{\mathrm{g}} + E_b(t) \cdot \eta_{\mathrm{b}} + E_{pv}(t) \cdot \eta_{\mathrm{pv}} = E_{load}(t) \tag{8}$$

being

$$E_b(t) = P_b(t) \cdot \Delta t = V_t(t) \cdot I_b(t) \cdot \Delta t$$

$$E_{pv}(t) = P_{pv}(t) \cdot \Delta t$$

$$E_{load}(t) = P_{load}(t) \cdot \Delta t$$

where E_g is the energy supplied by the utility grid; E_b represents the input or output energy of the BESS; E_{pv} is the predicted energy generated by the PV system; E_{load} stands for the forecasting energy demand of the consumer; η_{g} η_{b} and η_{pv} are the efficiencies of the converters; P_b, P_{pv}, and P_{load} are the power of the BESS, PV, and loads respectively.

Furthermore, since there are two operational modes of the BESS: charge and discharge, E_b can, therefore, be written as follows:

$$E_b(t) = \begin{cases} E_i(t) \cdot \eta_d(I) & \text{when discharging} \\ E_i(t) / \eta_c(I) & \text{when charging} \end{cases} \tag{9}$$

Accordingly, the internal energy of the BESS can be represented regarding its output energy as follows:

$$E_i(t) = E_i(t-1) - \Delta E_i(t) \tag{10}$$

being

$$\Delta E_i(t) = \begin{cases} P_b(t) \cdot \Delta t / \eta_d(t) & \text{when discharging} \\ P_b(t) \cdot \Delta t \cdot \eta_c(t) & \text{when charging} \end{cases}$$

where ΔE_i is internal energy variation during an optimizing interval; P_b is the input or output power of the BESS, and it is positive when BESS is discharged, and negative when BESS is charged by the PV or utility grid.

The stored energy inside the BESS should be maintained after a 24 hours' operation, so that the energy management for the next day may not be influenced. Therefore, the gross of the increment and decrement of the internal energy should be limited within 24 hours. Hence, the constraint can be given as follows:

$$\sum_{t=1}^{\mathrm{T}} \Delta E_i(t) = 0 \tag{11}$$

Additionally, considering the capability of the converters and batteries, the output and input powers of the energy sources should be limited.

a) For the grid, since selling electrical energy to the utility grid is forbidden. Thus the boundary for utility grid can be expressed as follows:

TABLE III

VALUE OF THE LIMITATION

Limitation	Symbol	Value
Maximum input power of the converter	P_{g_max}	8 kW
Maximum charging power of BESS	P_{bc_max}	10 kW
Maximum discharging power of BESS	P_{bd_max}	20 kW
Minimum SoC of the BESS	$SoC_{i,min}$	10 %
Maximum SoC of the BESS	$SoC_{i,max}$	100 %
Minimum internal energy of the BESS	E_{i_min}	2 kWh
Maximum internal energy of the BESS	E_{i_max}	30 kWh

$$0 \le P_g(t) \le P_{g\_max} \tag{12}$$

where P_{g_max} is the upper limit of the input power of the grid converter.

b) For the BESS, based on overall consideration of the allowed charge and discharge current rate of the battery and the rated power of the converter, the boundary is therefore given as follows:

$$P_{bc\_max} \le P_b(t) \le P_{bd\_max} \tag{13}$$

where P_{bc_max} is the maximum charging power of the BESS; P_{bd_max} is the maximum discharging power.

Furthermore, in order to prevent the battery from overcharge and over-discharge, the ranges of batteries' SoC and internal energy are set as:

$$SoC_{min} \le SoC(t) \le SoC_{max} \tag{14}$$

$$E_{i\_min} \le E_i(t) \le E_{i\_max} \tag{15}$$

where SoC_{min} and SoC_{max} are the lower and upper limits of the SoC; E_{i_min} and E_{i_max} are the bounds of the E_i.

In addition, the numerical values of the aforementioned bounds are shown in Table III.

C. Energy Management Strategy

By combining the equations proposed above, (7)-(15), the optimization problem can be described as follows:

$$\begin{aligned}
\min \quad & J_c = \sum_{t=1}^{T} P_g(t)\cdot\Delta t\cdot f_p(t) \\
\text{s.t.} \quad & P_g(t)\cdot\Delta t\cdot\eta_g + P_b(t)\cdot\Delta t\cdot\eta_b + P_{pv}(t)\cdot\Delta t\cdot\eta_{pv} = P_{load}(t)\cdot\Delta t \\
& \sum_{t=1}^{T}\Delta E_i(t) = 0 \\
& 0 \le P_g(t) \le P_{g_max} \\
& P_{bc_max} \le P_b(t) \le P_{bd_max} \\
& SoC_{min} \le SoC(t) \le SoC_{max} \\
& E_{i_min} \le E_i(t) \le E_{i_max}
\end{aligned} \tag{16}$$

Due to the two operation modes of the BESS, shown in (9) and (10), $P_b(t)$ is a non-smooth and nonlinear function in its domain of definition. Hence, the optimization problem of (16) should be treated as a DNLP problem.

A day-ahead scheduling approach for MG is developed based on the PV and loads forecasted data of next 24 hours in this paper. To minimize the electricity cost, the proposed DNLP

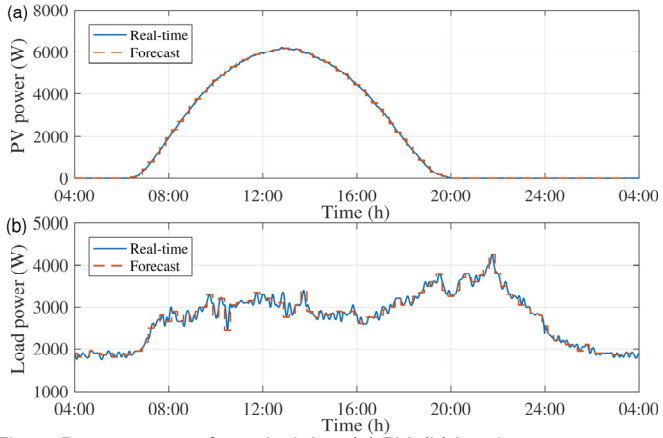

Fig. 5. Power curves of a typical day: (a) PV; (b) Load.

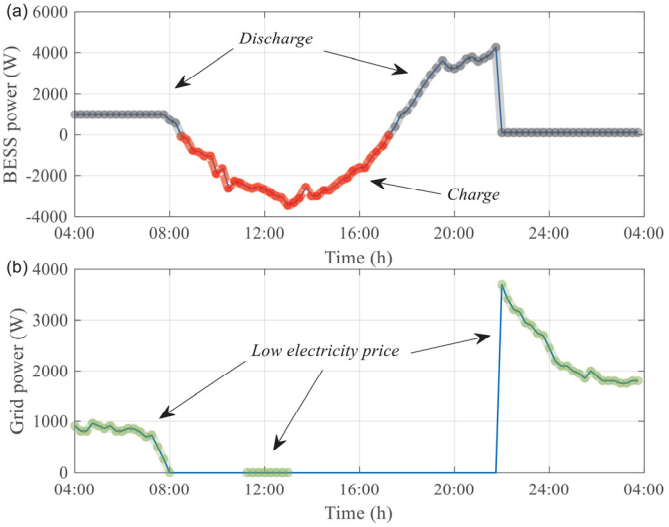

Fig. 6. Power schedule in 24 hours: (1) BESS; (2) Grid.

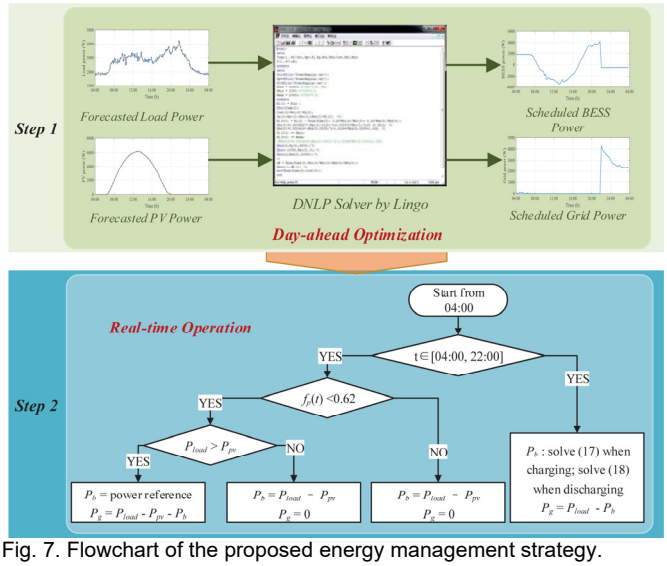

Fig. 7. Flowchart of the proposed energy management strategy.

This article has been accepted for publication in a future issue of this journal, but has not been fully edited. Content may change prior to final publication. Citation information: DOI 10.1109/TIE.2018.2818660, IEEE Transactions on Industrial Electronics

problem in (16) is solved by a comprehensive tool named Lingo which is designed for building and solving linear, nonlinear, quadratic problems and etc. [24]. Notice, any other optimization tools that can solve DNLP problem, can also be used to obtain the optimal results. The PV power data forecasted based on the weather forecasting and historical PV generation database is given in Fig. 5 (a). The blue line is the measured data, and the red one is the forecasting data. Moreover, the load's data is predicted based on the historic power demands of the consumer, as shown in Fig. 5 (b). As can be seen from Fig. 5, the total generation energy of the PV system is about 32 kWh in a typical day. Moreover, the energy demand is about 66 kWh within 24 hours.

In order to guarantee enough time for BESS charging within a low price period to maintain the internal energy, and reduce the impact of PV forecasting error on BESS operating power at the end of EMS operation period, therefore, the day-ahead power schedule is starting from 4 o'clock in the morning. Hence, after solving the DNLP problem in (16), optimal power references for each energy source would be obtained and sent from the EMS every 15 minutes. Scheduled powers of a typical day for BESS and utility grid are illustrated in Fig. 6. PV and loads power data from the Fig. 5 are utilized during this optimization. As can be seen from Fig. 6, the loads are supplied by the utility grid only in the low electricity price period. Energy from the PV system is completely delivered to the loads or BESS. However, due to the predicting errors of the PV and loads, as can be seen from Fig. 5, the scheduled power may not be appropriate for real-time operation of the MG. Thus, to address this issue, a flow diagram based on the 24-hour power schedule is then developed, shown in Fig. 7.

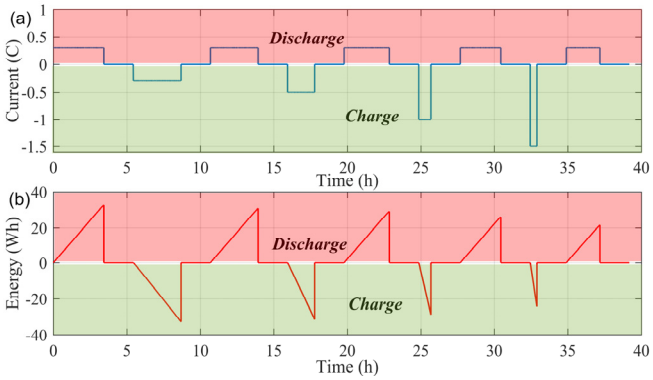

Fig. 8. Experiment for the verification of efficiencies with different charging currents: (a) Current; (b) Energy.

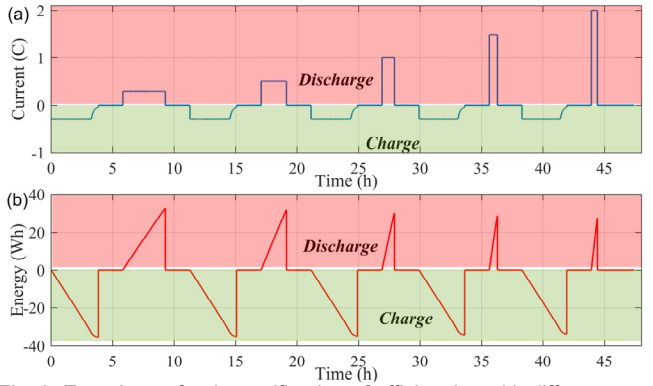

Fig. 9. Experiment for the verification of efficiencies with different discharging currents: (a) Current; (b) Energy.

As described in Fig. 7, power references of the BESS and grid were computed by the DNLP solver and transferred to the real-time operator. Afterwards, the MG is operating from 04:00 in the morning and working under the dispatching rule as follows. If the current time, t, is in the range of [04:00, 22:00], the electricity price is less than 0.62, and the demand power is bigger than PV power, the BESS will provide the power same as power reference. Moreover, the utility grid will supply the rest of the demand. If the load's power is not bigger than PV, the required power will be provided by the BESS and PV. Likely, BESS and PV should supply the loads when electricity price is higher than 0.62. As described in Section III, the internal energy of the BESS should be controlled to its initial value after 24 hours' operation. Therefore, in order to balance the internal energy, the output/input power of the BESS from 22:00 to 04:00 (next day) can be calculated by solving the equation as follows.

1) If the internal energy of the BESS at 22:00 was less than its initial value at 04:00, the BESS should be charged. The input power is obtained by solving the equation as follows.

$$\sum_{t=22:00}^{04:00}(\hat{P}_b(t)\cdot\eta_c(I_c)\cdot\tau)+\sum_{t=04:00}^{22:00}(P_b(t)\cdot\eta\cdot\tau)=0 \tag{17}$$

2) If the internal energy of the BESS was greater than the initial value, the output power of the BESS should satisfy the following equation.

$$\sum_{t=22:00}^{04:00}(\hat{P}_b(t)\cdot\tau \Big/ \eta_d(I_d))+\sum_{t=04:00}^{22:00}(P_b(t)\cdot\eta\cdot\tau)=0 \tag{18}$$

being

$$\eta=\begin{cases}1/\eta_d(t) & \text{when discharging}\\ \eta_c(t) & \text{when charging}\end{cases}$$

where $\hat{P}_b(t)$ is the input/output power of the BESS in the last 6 hours of the MG operating period; τ is the unitary time and is using the hour as unit; η is the energy storage efficiency of the battery. The increment or decrement of the BESS internal energy produced in the period of [04:00, 22:00] would be eliminated to zero by (17) and (18). Moreover, the utility grid may supply the remaining demand power of the loads together with BESS.

V. Experimental Results

To validate the proposed battery efficiency expression and the energy management strategy, some experiments are conducted.

A. Battery Efficiency Verification

A series of battery experiments have been designed to validate the lithium-ion battery energy storage efficiency with different charging and discharging currents. The experimental profiles are illustrated in Fig. 8 and 9.

In order to measure the efficiency of different charging current. A fully charged battery is firstly discharged with a

This article has been accepted for publication in a future issue of this journal, but has not been fully edited. Content may change prior to final publication. Citation information: DOI 10.1109/TIE.2018.2818660, IEEE Transactions on Industrial Electronics

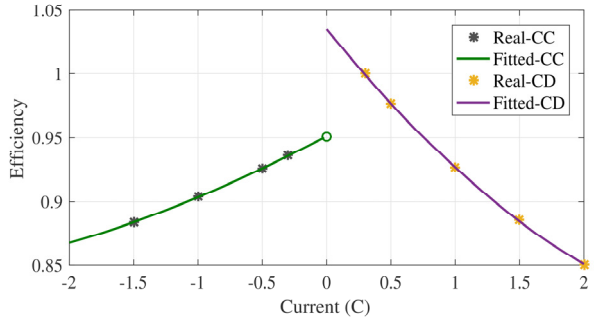

Fig. 10. The efficiency of the lithium-ion battery.

constant 0.3 C current. Then, the battery would have a 2 hours' rest. Afterwards, it is charged with a constant 0.3 C current until the terminal voltage reaching 3.65 V. In this charge and discharge circle, the energy storage efficiency at 0.3 C charging current is obtained by the discharged energy dividing the charged energy. Notice that, the discharged energy under constant 0.3 C is assumed to be the stored energy inside the battery in this paper. In other words, the discharged energy with 0.3 C is set as the reference for efficiency definition. Similarly, efficiencies of battery with 0.5 C, 1.0 C and 1.5 C charging current are therefore acquired through the current profile shown in Fig. 8 (a).

Moreover, battery storage efficiencies at different discharging current can be calculated based on the data using current profile in Fig. 9. The lithium-ion battery is fully charged with constant 0.3 C and constant 3.65 V charging at the beginning of every experimental circle. The only difference between each circle is the value of discharging current. 0.3 C, 0.5 C, 1.0 C, 1.5 C and 2.0 C discharging currents aare used in the experiment as shown in Fig. 9 (a). Charged and discharged energies are shown in Fig. 9 (b). As mentioned before, the efficiency in discharging process would be the discharged energy with a certain current divide the output energy with 0.3 C.

Battery storage efficiencies under different operating current are plotted in Fig. 10. The grey and yellow dots are the measured data from the experiment, and the green and blue curves are plotted after fitting. As analyzed in Section III, two quadratic polynomials are employed to formulate battery energy storage efficiencies and are given as follows.

$$\eta_c(I_c) = \mathrm{a} \cdot I_c^2 + \mathrm{b} \cdot I_c + \mathrm{c} \tag{19}$$

$$\eta_d(I_d) = \mathrm{d} \cdot I_d^2 + \mathrm{e} \cdot I_d + \mathrm{f} \tag{20}$$

where a, b, c, d, e, and f are the unknown parameters, and are identified based on the recursive least squares method and the experimental data.

B. Effect of the battery efficiency on EMS

To evaluate the proposed formulating approach, two kinds of common used approach for the formulation of battery energy storage efficiency are employed in a comparative experiment. For the first approach, battery efficiency is only determined by the charge/discharge state. In this approach, the energy storage efficiencies are two constants for the charging and discharging respectively. Moreover, in the second approach, the energy storage efficiencies during charging and discharging process are formulated with same equations. To fit the measured data in Fig. 10, the efficiency equation in [22] is modified as

$$\eta_s(I_b) = -0.08775 \cdot |I_b| + 1.021 \tag{21}$$

where η_s is the battery efficiency calculated by the second approach.

The numeral results of aforementioned approaches are compared in Table IV. As the table shows, the approach proposed in this paper is more accurate and appropriate for battery energy storage efficiency formulation than the common used approaches in previous studies.

To investigate the effect of different battery efficiency formulating approaches on the results of EMS, experiments of EMS using the aforementioned approaches and the approach proposed in this paper are conducted. PV generation and load profiles of a typical day, as shown in Fig. 5, are used in this experiment. The initial energy of the BESS is set to 15 kWh.

Power schemes of EMS using different battery efficiency formulating approaches are shown in Fig. 11. Scheduled power profiles of the BESS are given in Fig. 11 (a). It should be notice that these power profiles are the input/output power of the BESS in real operation. Fig. 11(b) shows the calculated and real internal energy of the BESS. The red line, green dashed line and blue dashed line are BESS' internal energy computed by the proposed approach in this paper. The green and blue solid lines are BESS internal energy calculated by the constant value efficiency and single equation efficiency respectively.

TABLE IV

COMPARISON RESULTS OF DIFFERENT APPROACHES FOR EFFICIENCY CALCULATION

Approach	Values of the battery energy storage efficiency under different situations					
	Charge under 0.3 C	Charge under 0.5 C	Charge under 1 C	Discharge under 0.3 C	Discharge under 0.5 C	Discharge under 1.5 C
Measured	0.9358	0.9255	0.9037	1	0.9765	0.886
Proposed (19), (20) in this paper	0.9356	0.9258	0.9035	0.9991	0.9768	0.8847
Constant value [1]	0.8	0.8	0.8	0.95	0.95	0.95
Single equation [2]	0.9947	0.9771	0.9332	0.9947	0.9771	0.8894

[1] Constant value means battery efficiencies are two constants during charging and discharging respectively.
[2] Single equation means equations for battery efficiency description during charging and discharging are the same.

This article has been accepted for publication in a future issue of this journal, but has not been fully edited. Content may change prior to final publication. Citation information: DOI 10.1109/TIE.2018.2818660, IEEE Transactions on Industrial Electronics

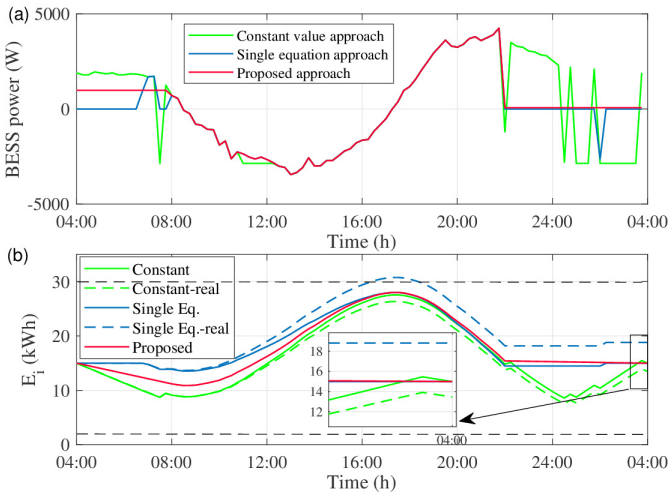

Fig. 11. Comparison of EMS using different efficiency equations: (a) BESS power; (b) Internal energy of BESS.

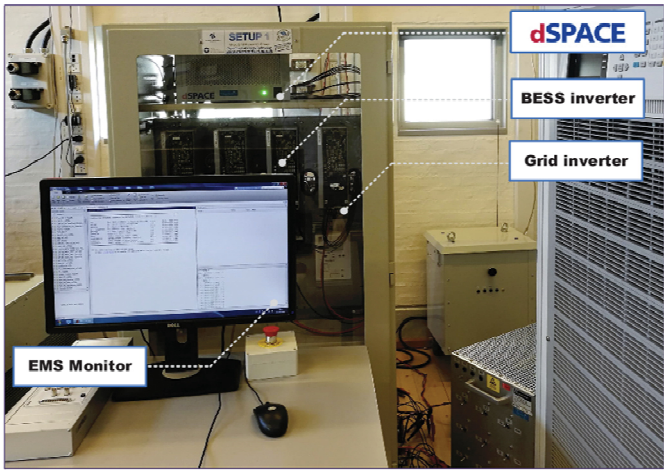

Fig. 12. Experimental platform.

Due to the errors of constant value and single equation approaches, the real internal energy of the BESS (dashed lines) may be lower or higher than the calculated value (solid lines). For example, the calculated internal energy is lower than the real value when the constant value efficiency is used during charging, as shown Fig. 11 (b).

As shown in Fig. 11 (b), after 24 hours' operation, the real internal energy may be higher than 15 kWh if the constant value efficiency was applied. Moreover, the internal energy may be lower by using the single equation efficiency. Both of these situations are not allowed according to the constraints. More importantly, the real internal energy would be higher or lower than the boundaries if an inaccurate battery efficiency has been used in the EMS. Thus, an accurate battery energy storage efficiency may help developing an appropriate energy management strategy of the MG, and also protecting the BESS from damages.

In summary, the proposed battery efficiency formulating approach in this paper is verified to be accurate for battery energy storage efficiency modeling and may be reliable for the EMS during power scheduling.

C. Experimental Results of the Proposed EMS

In order to validate the proposed energy management strategy, experiments under different predicting errors are conducted. To simplify the analysis, different forecasting errors of the PV power are only discussed. The predicting error is much bigger in *Case 2* than *Case 1*. The initial condition of SoC is set to 50%, and the initial stored energy of the BESS is about 15 kWh. The energy management strategy is modeled by Matlab/Simulink and implemented in a real-time platform, dSPACE 1006, as shown in Fig. 12. The PV and loads data are also downloaded to the dSPACE for simulation. The 1st order RC model is implemented on this platform to model the dynamic behavior of the BESS as well. Results of the MG operation is displayed on the monitor.

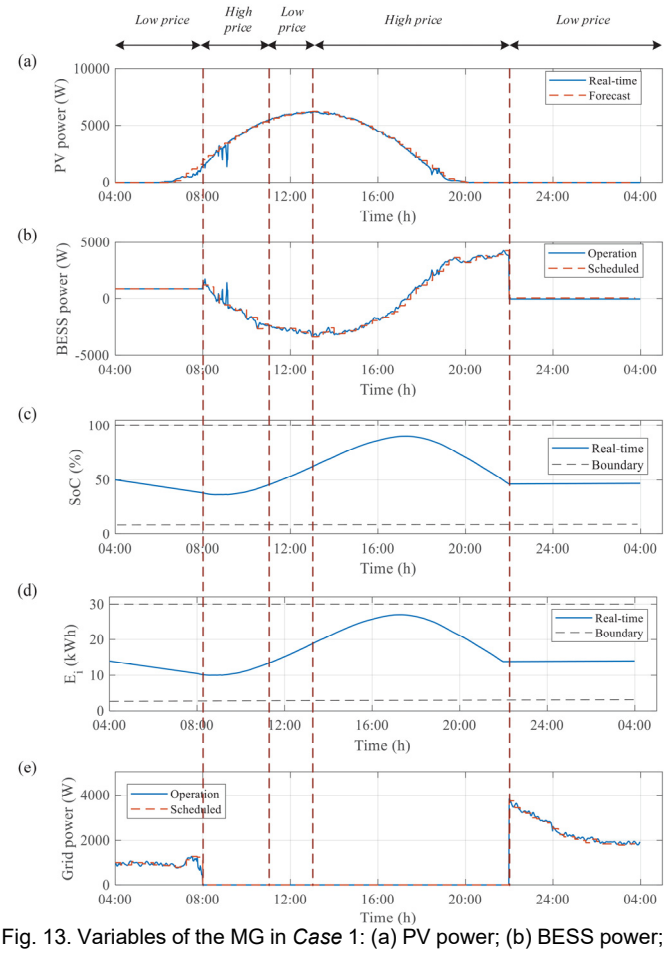

Fig. 13. Variables of the MG in *Case* 1: (a) PV power; (b) BESS power; (c) SoC; (d) Internal energy of BESS; (e) Grid power.

In *Case* 1, a PV power profile of a sunny day with small forecasting error is implemented, as shown in Fig. 13 (a). The mean absolute error (MAE) is 81.8410 W, and the mean squared error (MSE) is 3.6220e+4 W^2. Scheduled power of the BESS from the DNLP solver based on the forecast PV power is plotted as the red line in Fig. 13 (b). Moreover, the real-time operational power of the BESS is the blue line in Fig. 13 (b). The SoC and internal energy of the BESS are illustrated in Fig. 13 (c) and (d). The power supplied by the utility grid is shown in Fig. 13 (e).

During the operation of the MG, the maximum SoC is 89.73%, and the minimum SoC is about 36%. Moreover, the BESS is also working in the safe range of internal energy. In the 24-hour operating period, the total cost of the electricity is 11.4 CNY. However, if there were no PV and BESS, the total cost of

This article has been accepted for publication in a future issue of this journal, but has not been fully edited. Content may change prior to final publication. Citation information: DOI 10.1109/TIE.2018.2818660, IEEE Transactions on Industrial Electronics

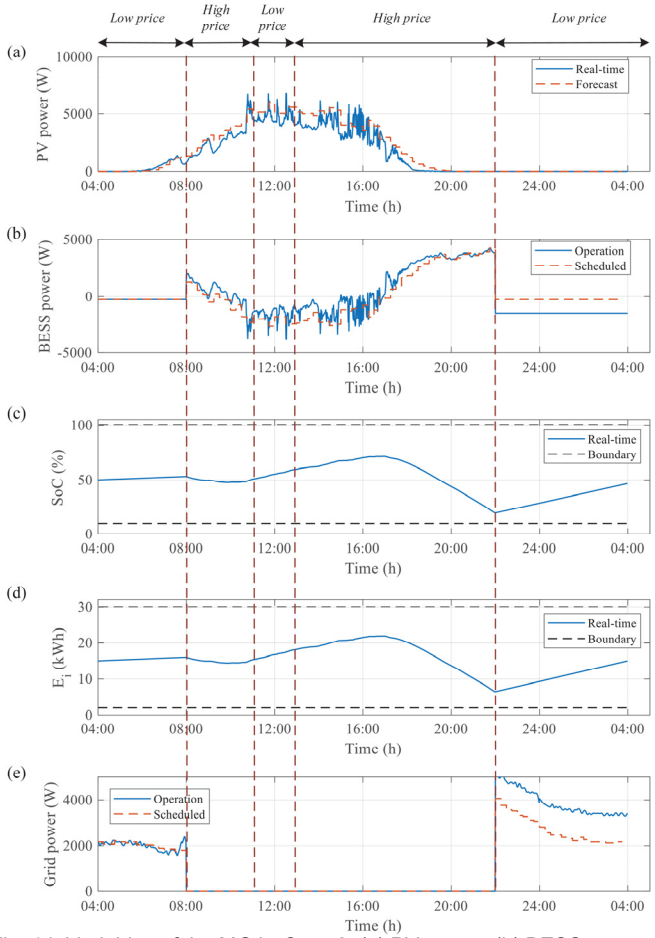

Fig. 14. Variables of the MG in *Case* 2: (a) PV power; (b) BESS power; (c) SoC; (d) Internal energy of BESS; (e) Grid power.

the loads would be 66.2 CNY. Furthermore, the cost may be about 32.9 CNY if there was no EMS.

In *Case* 2, a PV power profile of a cloudy day is applied in the HIL experiment. The PV power changes sharply from 11:00 to 18:00. As can be seen from the experimental result shown in Fig. 14, during the operational period, the curtailment of the renewable energy is guaranteed to be 0. The loads are supplied by the PV system and BESS when PV generation or electricity price is high. Otherwise, the utility grid and BESS are cooperating with each other to support the loads. During the operational process of the MG, the maximum SoC is 87.36%, and the minimum is 38.38%. Moreover, the utility grid is always working with low electricity price.

In the 24-hour HIL experiment, the total cost of the MG using the proposed energy management strategy is 19.4 CNY. The total cost of MG without PV and BESS is same as the cost in *Case* 1, which is 66.2 CNY. Moreover, if there were no EMS, the total cost of the MG would be 37.1 CNY, which would be 1.9 times higher than the one using the proposed approach.

As can be seen from the HIL experimental results in Fig. 13 and Fig. 14, the forecasting errors may directly influence the optimizing results of the EMS. If the MG was operating under a small forecasting error, like *Case I*, the operating power of the BESS and main grid would be more similar to the day-ahead scheduled power references than the MG under large forecasting errors do. In *Case I*, the total cost of the real time operation is 11.4 CNY, and the total cost of the scheduled power is 11.3 CNY. However, due to the larger forecasting error, the difference of total cost between the real time operation and power schedule is 4.5 CNY in *Case II*. This is mainly caused by the BESS charging during the last 6 hours since the internal energy of the BESS has been used for power compensation from 8:00 to 22:00. However, even the forecasting errors may impact the operating results, the proposed energy management strategy can still help reducing the electricity cost of the grid-tied MG by optimizing the power flow and efficiency, and scheduling the BESS and utility grid. The experimental results also show that the proposed method can protect the BESS from over-charging and over-discharging, and take advantage of the RES.

VI. Conclusion

An energy management strategy considering the energy storage efficiency of the BESS has been developed in this paper to minimize the electricity cost of a grid-tied AC MG. The energy storage efficiency formulas of the lithium-ion battery were qualitatively analyzed based on battery electrical properties and quantificationally verified by different charge/discharge experiments. Furthermore, the proposed battery efficiency equations were validated through the comparative experiment. Moreover, these equations were employed within the modeling of MG which was aiming to obtain an optimal schedule of the power flow. Besides, the optimization issue in this paper is addressed by the DNLP solver from Lindo. Based on the schemed power reference of the sub-systems in the MG, a two-step energy management strategy of the MG was then proposed. The HIL experiment has been applied to validate the proposed MG energy management approach. It is possible to conclude that the proposed energy management strategy can reduce the electricity cost of the MG, even with different forecasting errors of the RESs.

References

[1] J. M. Guerrero, P. C. Loh, T. L. Lee, and M. Chandorkar, "Advanced Control Architectures for Intelligent Microgrids—;Part II: Power Quality, Energy Storage, and AC/DC Microgrids," *IEEE Transactions on Industrial Electronics,* vol. 60, pp. 1263-1270, 2013.

[2] D. E. Olivares, A. Mehrizi-Sani, A. H. Etemadi, C. A. Cañizares, R. Iravani, M. Kazerani*, et al.*, "Trends in Microgrid Control," *IEEE Transactions on Smart Grid,* vol. 5, pp. 1905-1919, 2014.

[3] J. C. Vasquez, J. M. Guerrero, J. Miret, M. Castilla, and L. G. d. Vicuna, "Hierarchical Control of Intelligent Microgrids," *IEEE Industrial Electronics Magazine,* vol. 4, pp. 23-29, 2010.

[4] L. Meng, T. Dragicevic, J. Roldán-Pérez, J. C. Vasquez, and J. M. Guerrero, "Modeling and Sensitivity Study of Consensus Algorithm-Based Distributed Hierarchical Control for DC Microgrids," *IEEE Transactions on Smart Grid,* vol. 7, pp. 1504-1515, 2016.

[5] W. Feng, K. Sun, Y. Guan, J. Guerrero, and X. Xiao, "Active Power Quality Improvement Strategy for Grid-connected Microgrid Based on Hierarchical Control," *IEEE Transactions on Smart Grid,* vol. PP, pp. 1-1, 2017.

[6] X. Liu, J. Wu, C. Zhang, and Z. Chen, "A method for state of energy estimation of lithium-ion batteries at dynamic currents and temperatures," *Journal of Power Sources,* vol. 270, pp. 151-157, 2014.

[7] J. Wu, C. Zhang, and Z. Chen, "An online method for lithium-ion battery remaining useful life estimation using importance sampling and neural networks," *Applied Energy,* vol. 173, pp. 134-140, 2016.

[8] J. Wu, Y. Wang, X. Zhang, and Z. Chen, "A novel state of health estimation method of Li-ion battery using group method of data handling," *Journal of Power Sources,* vol. 327, pp. 457-464, 2016.

[9] J. Meng, G. Luo, and F. Gao, "Lithium Polymer Battery State-of-Charge Estimation Based on Adaptive Unscented Kalman Filter and Support Vector Machine," *IEEE Transactions on Power Electronics,* vol. 31, pp. 2226-2238, 2016.
[10] Y. Wang, C. Zhang, and Z. Chen, "A method for joint estimation of state-of-charge and available energy of LiFePO4 batteries," *Applied Energy,* vol. 135, pp. 81-87, 2014.
[11] G. Dong, X. Zhang, C. Zhang, and Z. Chen, "A method for state of energy estimation of lithium-ion batteries based on neural network model," *Energy,* vol. 90, pp. 879-888, 2015.
[12] J. Wei, G. Dong, Z. Chen, and Y. Kang, "System state estimation and optimal energy control framework for multicell lithium-ion battery system," *Applied Energy,* vol. 187, pp. 37-49, 2017.
[13] X. Hu, R. Xiong, and B. Egardt, "Model-Based Dynamic Power Assessment of Lithium-Ion Batteries Considering Different Operating Conditions," *IEEE Transactions on Industrial Informatics,* vol. 10, pp. 1948-1959, 2014.
[14] S. Chakraborty, M. D. Weiss, and M. G. Simoes, "Distributed Intelligent Energy Management System for a Single-Phase High-Frequency AC Microgrid," *IEEE Transactions on Industrial Electronics,* vol. 54, pp. 97-109, 2007.
[15] A. Chaouachi, R. M. Kamel, R. Andoulsi, and K. Nagasaka, "Multiobjective Intelligent Energy Management for a Microgrid," *IEEE Transactions on Industrial Electronics,* vol. 60, pp. 1688-1699, 2013.
[16] S. Beer, T. Gomez, D. Dallinger, I. Momber, C. Marnay, M. Stadler, *et al.*, "An Economic Analysis of Used Electric Vehicle Batteries Integrated Into Commercial Building Microgrids," *IEEE Transactions on Smart Grid,* vol. 3, pp. 517-525, 2012.
[17] C. Chen and S. Duan, "Optimal Integration of Plug-In Hybrid Electric Vehicles in Microgrids," *IEEE Transactions on Industrial Informatics,* vol. 10, pp. 1917-1926, 2014.
[18] T. Y. Lee, "Operating Schedule of Battery Energy Storage System in a Time-of-Use Rate Industrial User With Wind Turbine Generators: A Multipass Iteration Particle Swarm Optimization Approach," *IEEE Transactions on Energy Conversion,* vol. 22, pp. 774-782, 2007.
[19] D. E. Olivares, C. A. Cañizares, and M. Kazerani, "A Centralized Energy Management System for Isolated Microgrids," *IEEE Transactions on Smart Grid,* vol. 5, pp. 1864-1875, 2014.
[20] L. Meng, T. Dragicevic, J. C. Vasquez, and J. M. Guerrero, "Tertiary and Secondary Control Levels for Efficiency Optimization and System Damping in Droop Controlled DC–DC Converters," *IEEE Transactions on Smart Grid,* vol. 6, pp. 2615-2626, 2015.
[21] J. Liu, H. Chen, W. Zhang, B. Yurkovich, and G. Rizzoni, "Energy Management Problems Under Uncertainties for Grid-Connected Microgrids: a Chance Constrained Programming Approach," *IEEE Transactions on Smart Grid,* vol. 8, no. 6, pp. 2585-2596, 2017.
[22] Q. Wei, D. Liu, F. L. Lewis, Y. Liu, and J. Zhang, "Mixed Iterative Adaptive Dynamic Programming for Optimal Battery Energy Control in Smart Residential Microgrids," *IEEE Transactions on Industrial Electronics,* vol. 64, pp. 4110-4120, 2017.
[23] X. Hu, S. Li, H. Peng, and F. Sun, "Robustness analysis of State-of-Charge estimation methods for two types of Li-ion batteries," *Journal of Power Sources,* vol. 217, pp. 209-219, 2012.
[24] LINDO Systems, Inc., (2017). [Online]. Available: https://www.lindo.com/index.php/products/lingo-and-optimization-modeling

Ji Wu (S'15) received the B.E. degree in Automation from the Hefei University of Technology, Hefei, China, in 2011. He is currently working toward the Ph.D. degree at the Department of Automation, University of Science and Technology of China, Hefei, China.

From 2016 to 2017, he was a guest Ph.D. student with the Department of Energy Technology, Aalborg University, Aalborg, Denmark. His areas of research are the modeling, control and optimization of the complex systems, including battery energy storage systems, electric vehicles and microgrids.

Xiaowen Xing was born in Xi'an, China, in February 1985. She received her B.S. degree from the Secondary Artillery Engineering University, Xi'an, China, and the M.E. degree from the Xi'an University of Technology, Xi'an, China, in 2008 and 2013, respectively. From 2016 to 2017, she was a guest Ph.D. student with the Department of Energy Technology, Aalborg University, Aalborg, Denmark. She is currently working toward the Ph.D. degree in electrical engineering at Northwestern Polytechnical University, Xi'an, China.

Her main research interests include microgrid cluster, energy management, and power converters.

Xingtao Liu was born in Hebei, China, in December 1985. He received the B.E. degree in automation and the Ph.D. degree in information acquisition and control from the University of Science and Technology of China, Hefei, China, in 2009 and 2014, respectively.

He has been an associate professor in the School of Automotive and Traffic Engineering, Hefei University of Technology, Hefei, China, since 2017. His main research interests include modeling and control of complex system, intelligent vehicle, and energy management technologies for electric vehicles.

Josep M. Guerrero (S'01-M'04-SM'08-FM'15) received the B.S. degree in telecommunications engineering, the M.S. degree in electronics engineering, and the Ph.D. degree in power electronics from the Technical University of Catalonia, Barcelona, in 1997, 2000 and 2003, respectively.

Since 2011, he has been a Full Professor with the Department of Energy Technology, Aalborg University, Denmark, where he is responsible for the Microgrid Research Program (www.microgrids.et.aau.dk). His research interests are oriented to different microgrid aspects, including power electronics, distributed energy-storage systems, hierarchical and cooperative control, energy management systems, smart metering and the internet of things for AC/DC microgrid clusters and islanded minigrids.

Prof. Guerrero is an Associate Editor for a number of IEEE TRANSACTIONS. He received the best paper award of the IEEE Transactions on Energy Conversion for the period 2014-2015, and the best paper prize of IEEE-PES in 2015. As well, he received the best paper award of the Journal of Power Electronics in 2016. In 2014, 2015, 2016, and 2017 he was awarded by Thomson Reuters as Highly Cited Researcher, and in 2015 he was elevated as IEEE Fellow for his contributions on "distributed power systems and microgrids."

Zonghai Chen (M'17) was born in Anhui, China, in December 1963. He received the B.S. degree and the M.E. degree from the University of Science and Technology of China (USTC), Hefei, China, in 1988 and 1991, respectively.

He has been a Professor with the Department of Automation, USTC, since 1998. His main research interests include modeling and control of complex systems, intelligent robotic and information processing, energy management technologies for electric vehicles and smart microgrids.

Prof. Chen is a recipient of special allowances from the State Council of PR China. He is a member of the Robotics Technical Committee and Modelling, Identification and Signal Processing Technical Committee of the International Federation of Automation Control (IFAC).